Phosphine-Based Dinuclear Platinum(II) Diamido, Amido−Hydroxo, Oxo−Amido, Oxo−Imido, Diimido, and Dihydrazido Complexes[1]

Jian Jun Li, Wei Li, Alan J. James, Todd Holbert, Tristan P. Sharp, and Paul R. Sharp*

Department of Chemistry, University of Missouri—Columbia, Columbia, Missouri 65211

Received October 23, 1998

The platinum(II) amido−hydroxo and diamido complexes $[(L_2Pt)_2(\mu\text{-NHR})(\mu\text{-OH})](BF_4)_2$ (**1**) (L = PPh_3, R = Ph, *p*-tol, *p*-$Bu^tC_6H_4$, *p*-$NO_2C_6H_4$; L_2 = dppp, R = Ph, *p*-tol) and $[L_2Pt(\mu\text{-NHR})]_2(BF_4)_2$ (**2**) (L_2 = dppm, R = H, Ph, *p*-tol, NH_2; L_2 = dppe, R = H, Ph, *p*-tol; L_2 = dppp, R = H, NH_2; L_2 = dppb, R = NH_2; L = PMe_2Ph, R = H) are prepared from the reaction of $[L_2Pt(\mu\text{-OH})]_2(BF_4)_2$ with NH_2R. $[(PPh_3)_4Pt_2(\mu\text{-OH})(\mu\text{-NHR})](OTf)_2$ (R = *p*-$NO_2C_6H_4$) (**1a**), the triflate analogue of **1** (L = PPh_3, R = *p*-$NO_2C_6H_4$), is similarly prepared from $[L_2Pt(OH_2)_2](OTf)_2$. Crystals of **1**·CH_2Cl_2 (L = PPh_3, R = *p*-tol) from CH_2Cl_2/ether are monoclinic ($P2_1/n$) with a = 16.331(5) Å, b = 23.908(5) Å, c = 19.233(6) Å, β = 99.01(1)°, and Z = 4. The cationic portion consists of two edge-shared square-planar Pt centers folded at the edge with *cis*-phosphines and bridging hydroxo and amido groups. $LiN(SiMe_3)_2$, $LiNPr^i_2$, LiPh, or LiMe addition to **1** (L = PPh_3, R = Ph, *p*-tol, *p*-$Bu^tC_6H_4$) or **1a** deprotonates the hydroxo group, forming the amido−oxo complexes $[(L_2Pt)_2(\mu\text{-NHR})(\mu\text{-O})](BF_4)$ (**3**) (L = PPh_3, R = Ph, *p*-tol, *p*-$Bu^tC_6H_4$) or $[(PPh_3)_4Pt_2(\mu\text{-O})(\mu\text{-NHR})](OTf)$ (L = PPh_3, R = *p*-$NO_2C_6H_4$) (**3a**). Deprotonation of the diamido complexes **2** (L_2 = dppm, R = H, Ph, *p*-tol, NH_2) with $LiN(SiMe_3)_2$ yields $[(dppm\text{-}H)Pt(\mu\text{-NHR})]_2$ (**4**) (R = H, Ph, *p*-tol) or $[(dppm\text{-}H)_2Pt_2(\mu\text{-}NHNH_2)_2Li(THF)_2]BF_4$ (**5**). Crystals of **4** (R = Ph) from CH_2Cl_2/ether are (183 K) orthorhombic ($Pna2_1$) with a = 38.272(2) Å, b = 9.2841(5) Å, c = 15.0099(7) Å, and Z = 4. The structure consists of two edge-shared square-planar Pt centers folded at the edge with syn-bridging amido groups and chelating dppm-H ligands. Crystals of **5**·5THF from THF are (183 K) monoclinic ($P2_1/n$) with a = 17.669(5) Å, b = 31.884(3) Å, c = 14.686(4) Å, β = 105.03(1)°, and Z = 4. The structure of the cationic portion shows two edge-shared square-planar Pt centers folded at the edge with syn-bridging $NHNH_2$ groups and chelating dppm-H ligands. The $NHNH_2$ groups bridge the Pt centers through the NH portion. The NH_2 portions coordinate to a $Li(THF)_2^+$ group in a "tweezers" fashion resulting in tetrahedral coordination about the Li atom. Further deprotonation of **4** with LiMe yields the anionic diimido complexes $[(dppm\text{-}H)Pt(\mu\text{-NR})]_2(Li)_2$ (**6**) (R = H, Ph, *p*-tol).

Introduction

The importance of the chemistry of late transition metal (groups 9−11) bonds to the anionic oxygen and nitrogen ligands oxo (O^{2-}), imido (RN^{2-}), amido (R_2N^-), and alkoxo/hydroxo (RO^-) is becoming increasingly recognized.[2] Many critical processes are catalyzed by late transition metals. These ligands, or closely related species, bonded to metal complexes or metal surfaces are thought to be involved.[3−6] The Wacker process[7] and ethylene epoxidation on Ag[3] are two well-known examples where the mechanisms are still topics of debate despite many years of study.

The antitumor activity of *cis*-$(NH_3)_2PtCl_2$ (*cis*-platin) and related complexes where hydrolysis is an important step in the activity of the drugs has spurred investigation into hydroxo Pt(II) and Pd(II) chemistry.[8] The reaction of molecular oxygen with Cu(I) complexes, of long-time interest in catalytic systems, has been advanced by interest in modeling Cu-containing proteins.[5,9] There is also general biological interest in metal bonds to nitrogen and oxygen because of their involvement in other biological systems including nitrogenase[10] and photosys-

(1) Late Transition Metal Oxo and Imido Complexes. 19. Part 18: Shan, H.; James, A. J.; Sharp, P. R. *Inorg. Chem.* **1998**, *37*, 5727−5732.

(2) Reviews: Bergman, R. G. *Polyhedron* **1995**, *14*, 3227−3237. Bryndza, H. E.; Tam, W. *Chem. Rev.* **1988**, *88*, 1163−1188. Fryzuk, M. D.; Montgomery, C. D. *Coord. Chem. Rev.* **1989**, *95*, 1−40. Lappert, M. F.; Power, P. P.; Sanger, A. R.; Srivastava, R. C. *Metal and Metalloid Amides: Synthesis, Structures, and Physical and Chemical Properties*; Ellis Horwood: Chichester, U.K., 1980. West, B. O. *Polyhedron* **1989**, *8*, 219−274. Gilje, J. W.; Roesky, H. W. *Chem. Rev.* **1994**, *94*, 895−910. Griffith, W. P. *Coord. Chem. Rev.* **1970**, *5*, 459−517. Sharp, P. R. *Comments Inorg. Chem.*, in press.

(3) Madix, R. J.; Roberts, J. T. In *Surface Reactions*; Madix, R. J., Ed.; Springer-Verlag: New York, 1994; pp 5−53.

(4) Taylor, K. C. *Catal. Rev. Sci. Eng.* **1993**, *35*, 457−450. Schmatloch, V.; Kruse, N. *Surf. Sci.* **1992**, *269/270*, 488−480. Lee, S. *Methanol Synthesis and Technology;* CRC Press: Boca Raton, FL, 1990. Cheng, W. H.; Kung, H. H. *Methanol Production and Use;* Marcel Dekker: New York, 1994. Jones, P. M.; May, J. A.; Reitz, J. B.; Solomon, E. I. *J. Am. Chem. Soc.* **1998**, *120*, 1506−1516. *Oxygen Complexes and Oxygen Activation by Transition Metals;* Plenum: New York, 1988. Guo, X.-C.; Madix, R. J. *J. Am. Chem. Soc.* **1995**, *117*, 5523−5530.

(5) Karlin, K. D.; Gultneh, Y. *Prog. Inorg. Chem.* **1987**, *35*, 219−328.

(6) Recent examples: Driver, M. S.; Hartwig, J. F. *J. Am. Chem. Soc.* **1996**, *118*, 7217−7218. Mann, G.; Hartwig, J. F. *J. Org. Chem.* **1997**, *62*, 5413−5418. Hartwig, J. F. *Syn. Lett.* **1997**, *3*, 329. Louie, J.; Driver, M. S.; Hamann, B. C.; Hartwig, J. F. *J. Org. Chem.* **1997**, *62*, 1268−1273. Wolfe, J. P.; Wagaw, S.; Marcoux, J. F.; Buchwald, S. L. *Acc. Chem. Res.* **1998**, *31* (12), 805−818. Marcoux, J. F.; Doye, S.; Buchwald, S. L. *J. Am. Chem. Soc.* **1997**, *119* (43), 10539−10540.

(7) Hamed, O.; Henry, P. M. *Organometallics* **1997**, *16*, 4903−4909. Backvall, J.-E.; Bjorkman, E. E.; Pettersson, L.; Siegbahn, P. *J. Am. Chem. Soc.* **1984**, *106*, 4369−4373. Backvall, J.-E.; Bjorkman, E. E.; Pettersson, L.; Siegbahn, P. *J. Am. Chem. Soc.* **1985**, *107*, 7265−7267.

(8) *Platinum, Gold, and Other Metal Chemotherapeutic Agents: Chemistry and Biochemistry*; American Chemical Society: Washington, D.C., 1983. Sherman, S. E.; Lippard, S. J. *Chem. Rev.* **1987**, *87*, 1153−1181.

10.1021/ic981246w CCC: $18.00
Published on Web 03/11/1999

tem II.[11] Although these systems contain middle or early transition metals, their chemistry is still sufficiently mysterious that late transition metal complexes can give valuable insight into the workings of the biological systems.

Finally, there is a more fundamental interest in late transition metal−nitrogen and −oxygen bonds, especially those involving the "soft" transition metals of the second and third series. Hard/soft acid/base theory[12] predicts an unfavorable interaction, suggesting relatively weak bonds and high reactivity. Studies challenge the supposition about weak bonding and suggest that in general M−O and M−N bonds for these metals are as strong as analogous M−C bonds.[13]

Our interest in late transition metal chemistry is focused on the second- and third-row metals Rh, Ir, Pd, Pt, Ag, and Au and primarily involves oxo (O^{2-}) and imido (RN^{2-}) complexes.[1,14,15] However, our major synthetic route to these complexes involves deprotonation of the corresponding hydroxo (OH^-) and amido (RNH^-) complexes. Thus, we are interested in the acid/base chemistry of these conjugate acid/base pairs. In addition, as has been pointed out by Driver and Hartwig,[16] the acid/base properties of the synthetically important alkali metal analogues is fundamental to their chemistry and should be expected to be similarly important for the transition metal complexes. Here we report a series of Pt(II) primary aryl amido complexes prepared by aminolysis of the corresponding hydroxo complexes. Deprotonation of these complexes was explored with the goal of increasing our understanding of ancillary ligand effects on the acid/base chemistry of these Pt(II) complexes. We have also isolated mixed amido−hydroxo complexes and unique dihydrazido complexes and explored their deprotonation chemistry.

Results

Amido Complexes. The amine reaction product of the hydroxo complexes $[L_2Pt(\mu\text{-OH})]_2(BF_4)_2$[17−19] depends on the identity of L and the amine. When L = PPh_3 or dppp, even large amounts of aryl amines give only single substitution of the OH group and the white to yellow amido−hydroxo complexes, $[(L_2Pt)_2(\mu\text{-NHR})(\mu\text{-OH})](BF_4)_2$ (**1**) (L = PPh_3, R = Ph, *p*-tol, *p*-Bu^{t}C$_6$H$_4$, *p*-$NO_2C_6H_4$; L_2 = dppp, R = Ph, *p*-tol),[20] are isolated in high yield (eq 1). A similar reaction

$$[L_2Pt(\mu\text{-OH})]_2(BF_4)_2 + RNH_2 \rightarrow \underset{\mathbf{1}}{[(L_2Pt)_2(\mu\text{-NHR})(\mu\text{-OH})](BF_4)_2} + H_2O \quad (1)$$

starting from $[(Ph_3P)_2Pt(OH_2)_2](OTf)_2$ yields $[\{(Ph_3P)_2Pt\}_2\{\mu\text{-NH}(p\text{-}NO_2C_6H_4)\}(\mu\text{-OH})](OTf)_2$ (**1a**), the triflate analogue of **1** (L = PPh_3, R = *p*-$NO_2C_6H_4$). Replacement of the second hydroxo group in **1** does not occur even in molten *p*-toluidene at 70 °C. Only the monosubstitution product **1** (L = PPh_3, R = *p*-tol) is obtained.

With a different set of phosphine hydroxo complexes, and for the dppp hydroxo complex with NH_3 and hydrazine, disubstitution does occur to give diamido complexes **2** (eq 2, R = H, L_2 = dppm, dppe, dppp, $2PMe_2Ph$; R = Ph, *p*-tol, L_2 = dppm, dppe; R = NH_2, L_2 = dppm, dppp, dppb).

$$[L_2Pt(\mu\text{-OH})]_2(BF_4)_2 + 2RNH_2 \rightarrow \underset{\mathbf{2}}{[L_2Pt(\mu\text{-NHR})]_2(BF_4)_2} + 2H_2O \quad (2)$$

^{31}P NMR spectra of the amido−hydroxo complexes **1** and **1a** show two doublets, one for the phosphine trans to the OH group and one for the phosphine trans to the NHR group. The *P*−P coupling is ca. 20 Hz, consistent with a *cis*-phosphine geometry at the Pt centers. Shifts for the bidentate phosphine complexes are also consistent with phosphine ligand chelation.[21] Each phosphine doublet displays the expected ^{195}Pt satellites. The upfield doublet shows larger P−Pt coupling than the downfield doublet, and the coupling constant is similar to that of the starting hydroxo complex. Since coupling constants depend on the donor strength of the ligand trans to the phosphine,[22] we assign this signal to the phosphorus atom trans to the OH group. ^{1}H NMR spectra show, in addition to signals for the phosphine ligand, a pair of singlets for the OH and NH groups in the range 5.90 to −1.10 ppm. No attempt was made to differentiate between OH and NH ^{1}H NMR peaks. (With other late transition metal amido−hydroxo complexes, either only one peak was observed[23,24] or, if two peaks were observed, they were not assigned.[16,25]) IR spectra show two bands, one in the range 3543−3563 cm^{-1}, assigned to the OH group, and the other in the range 3233−3294 cm^{-1}, assigned to the NH group.

The solid state structure of the amido−hydroxo complex **1** (L = PPh_3, R = *p*-tol) was determined by X-ray crystallography. An ORTEP diagram of the cationic portion is shown in Figure 1 and an abbreviated summary of crystal data and data collection and processing is given in Table 1. Selected bond distances and angles are listed in Table 2. The cationic portion of

(9) Karlin, K. D.; Tyeklar, Z. *Adv. Inorg. Biochem.* **1994**, *9*, 123−172. Solomon, E. I.; Baldwin, M. J.; Lowery, M. D. *Chem. Rev.* **1992**, *92*, 521−542. Solomon, E. I.; Tuczek, F.; Root, D. E.; Brown, C. A. *Chem. Rev.* **1994**, *94*, 827−856. Halfen, J. A.; Mahapatra, S.; Wilkinson, E. C.; Kaderli, S.; Young, V. G., Jr.; Que, L., Jr.; Zuberbuhler, A. D.; Tolman, W. B. *Science* **1996**, *271*, 1397−1400.
(10) *Molybdenum Enzymes, Cofactors and Model Systems*; American Chemical Society: Washington, D.C., 1993.
(11) Debus, R. J. *Biochem. Biophys. Acta* **1992**, *1102*, 269−352. Rutherford, A. W. *Trends Biochem. Sci.* **1989**, *14*, 227−232. Manchanda, R.; Brudvig, G. W.; Crabtree, R. H. *Coord. Chem. Rev.* **1995**, *144*, 1−38.
(12) Pearson, R. G. *J. Chem. Educ.* **1968**, *45*, 643. Pearson, R. G. *J. Am. Chem. Soc.* **1963**, *85*, 3533.
(13) Bryndza, H. E.; Fong, L. K.; Paciello, R. A.; Tam, W.; Bercaw, J. E. *J. Am. Chem. Soc.* **1987**, *109*, 1444−1456. Bryndza, H. E.; Domaille, P. J.; Tam, W.; Fong, L. K.; Paciello, R. A.; Bercaw, J. E. *Polyhedron* **1988**, *7*, 1441−1452.
(14) Ramamoorthy, V.; Sharp, P. R. *Inorg. Chem.* **1990**, *29*, 3336−3338.
(15) Li, W.; Barnes, C. L.; Sharp, P. R. *J. Chem. Soc., Chem. Commun.* **1990**, 1634−1636.
(16) Driver, M. S.; Hartwig, J. F. *Organometallics* **1997**, *16*, 5706−5715.
(17) Li, J. J.; Li, W.; Sharp, P. R. *Inorg. Chem.* **1996**, *35*, 604−613.
(18) (a) Bushnell, G. W.; Dixon, K. R.; Hunter, R. G.; McFarland, J. J. *Can. J. Chem.* **1972**, *50*, 3694. (b) Wimmer, S.; Castan, P.; Wimmer, F. L.; Johnson, N. P. *J. Chem. Soc., Dalton Trans.* **1989**, 403−412. (c) Bushnell, G. W.; Dixon, K. R.; Hunter, R. G.; McFarland, J. J. *Can. J. Chem.* **1972**, *50*, 3694. (d) Wimmer, S.; Castan, P.; Wimmer, F. L.; Johnson, N. P. *J. Chem. Soc., Dalton Trans.* **1989**, 403−412.
(19) Bandini, A. L.; Banditelli, G.; Demartin, F.; Manaserro, M.; Minghetti, G. *Gazz. Chim. Ital.* **1993**, *123*, 417−423.
(20) Abbreviations: dppm = bis(diphenylphosphino)methane, dppe = bis(diphenylphosphino)ethane, dppp = bis(diphenylphosphino)propane, dppb = bis(diphenylphosphino)butane, dppm-H = bis(diphenylphosphino)methanide.
(21) Garrou, P. E. *Chem. Rev.* **1981**, *81*, 229−266.
(22) (a) Hartley, F. R. *The Chemistry of Platinum and Palladium*; Applied Science Publishers: London, U.K., 1973. (b) Appleton, T. G.; Clark, H. C.; Manzer, L. E. *Coord. Chem. Rev.* **1973**, *10*, 335. (c) Shustorovich, E. M.; Porai-Koshits, M. A.; Buslaer, Yu. A. *Coord. Chem. Rev.* **1975**, *17*, 1. (d) Allen, F. H.; Pidcock, A. *J. Chem. Soc. A* **1968**, 2700. (e) Grim, S. O.; Wheatland, D. A. *Inorg. Nucl. Chem. Lett.* **1968**, *4*, 187.
(23) Ruiz, J.; Martínez, M. T.; Vicente, C.; García, G.; López, G.; Chaloner, P. A.; Hitchcock, P. B. *Organometallics* **1993**, *12*, 4321−4326.
(24) Nutton, A.; Maitlis, P. M. *J. Chem. Soc., Dalton Trans.* **1981**, 2339−2341.
(25) Driver, M. S.; Hartwig, J. F. *J. Am. Chem. Soc.* **1996**, *118*, 4206−4207.

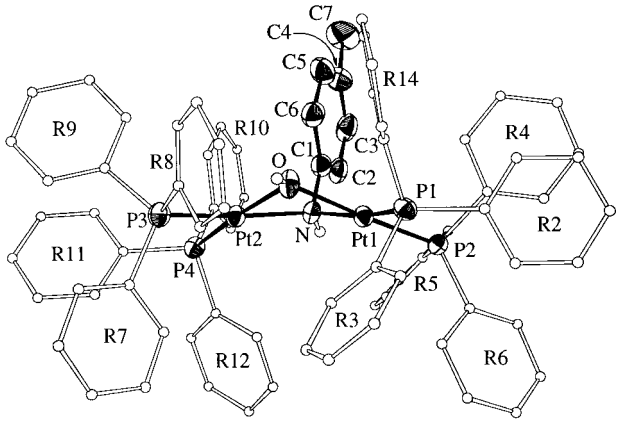

Figure 1. ORTEP drawing of the cationic portion of $[(L_2Pt)_2(\mu\text{-NHR})(\mu\text{-OH})](BF_4)_2$ (**1**) (L = PPh_3, R = *p*-tol).

the structure consists of two edge-shared square-planar Pt centers folded at the "hinge" edge with bridging OH and NHPh groups.

The higher symmetry of the diamido complexes **2** is reflected in their simpler ^{31}P NMR spectra. These show, like the parent hydroxo complexes,[17−19] singlets flanked by ^{195}Pt satellites. Smaller P−Pt coupling constants are observed for the diamido complexes, consistent with the greater donor strength of the amido ligand over the hydroxo ligand.[22] Shifts for the bidentate phosphine complexes indicate chelation.[21] Data for the PMe_2Ph and dppe complexes agree well with a previous report.[26]

^1H NMR signals for the NH groups of **2** are observed as broad singlets or triplets in the range 4.9−2.6 ppm for the R = Ph and *p*-tol derivatives and 1.2−1.7 ppm for the R = H derivatives. These shifts are relatively independent of solvent (DMSO-d_6, CD_2Cl_2, and $CDCl_3$) and are at lower field than those of the neutral diamido complexes $[LPtX(\mu\text{-}NH_2)]_2$ (L = PPh_3, PEt_3, PCy_3, $PMePh_2$, X = H, Me;[27] L = $PMePh_2$, X = $OPPh_2$[28]), which have NH_2 shifts upfield of TMS. Both of the dppm aryl derivatives (R = Ph, *p*-tol) of **2** show evidence of hindered rotation about the N−Ar bond. At ambient temperatures in $CDCl_3$ a series of four broad peaks are observed from 5.4 to 6.9 ppm in the spectrum of the *p*-tol derivative. These peaks are assigned to the four *p*-tol (MeC_6H_4) aromatic hydrogen atoms (ortho and meta), which are all unique in the absence of rotation. Rotation is faster in CD_2Cl_2, and the spectrum of the *p*-tol derivative shows only two broad peaks. Integration indicates that these may be assigned to equilibrating ortho and meta hydrogen atoms of the *p*-tol group. The Ph derivative shows similar behavior, but rotation is faster than in the *p*-tol derivative and only two overlapping broad peaks (ortho, meta, and para hydrogen atoms) are observed in CD_2Cl_2 and $CDCl_3$.

The dihydrazido complexes **2** (R = NH_2) show two peaks in their ^1H NMR spectra for the NH and NH_2 groups in a ratio of 1:2. For the dppm complex these are closely spaced at 4.0 and 3.8 ppm while the dppp and dppb complexes show greater separation with the NH peaks at 3.3 and 2.9 ppm and the NH_2 peaks at 1.2 and 1.3 ppm.

IR spectra of **2** show single bands in the 3231−3245 range for the R = Ph and *p*-tol derivatives. Two bands in the 3111−3359 cm^{-1} range separated by 100−200 cm^{-1} are observed for the R = H derivatives. These agree reasonably well with the values previously reported for the PMe_2Ph (3368, 3287 cm^{-1}) and the dppe (3357, 3265 cm^{-1}) complexes.[26] Differences may be assigned to the different media (mineral oil mull versus KBr disk). The hydrazido derivatives **2** (R = NH_2) show three NH bands, one in each of the three regions 3147−3154, 3231−3253, and 3290−3334 cm^{-1}.

Deprotonation Reactions. Addition of 1 equiv of $LiNPr^i_2$ to suspensions of $[(L_2Pt)_2(\mu\text{-NHR})(\mu\text{-OH})](BF_4)_2$ (**1**) (L = PPh_3) in THF gives homogeneous pale yellow solutions. ^{31}P NMR spectroscopy of the solutions shows a pair of doublets flanked by ^{195}Pt satellites similar to those of **1** but with different shifts and coupling constants. Workup gives pale orange crystals of $[(PPh_3)_4Pt_2(\mu\text{-NHR})(\mu\text{-O})](BF_4)$ (**3**) (R = Ph, *p*-tol, *p*-$Bu^tC_6H_4$, eq 3). $[(PPh_3)_4Pt_2(\mu\text{-NHR})(\mu\text{-O})](OTf)$ (R = *p*-$NO_2C_6H_4$) (**3a**)

$$[(PPh_3)_4Pt_2(\mu\text{-NHR})(\mu\text{-OH})](BF_4)_2 + LiNPr^i_2 \rightarrow \underset{\mathbf{1}\ (L = PPh_3)}{} [(PPh_3)_4Pt_2(\mu\text{-NHR})(\mu\text{-O})](BF_4) + LiBF_4 + HNPr^i_2 \quad (3)$$
$$\mathbf{3}$$

was similarly prepared from **1a**. Attempts to deprotonate **1** (L_2 = dppp) gave intractable mixtures.

^1H NMR spectra of **3** and **3a** show only one peak (2.40−2.80 ppm) that can be assigned to an NH or an OH group. IR spectra for **3** show an NH band at 3294−3299 cm^{-1}. The OH band of **1** and **1a** is absent, establishing that **3** and **3a** result from deprotonation of the OH group. Complex **3** (R = Ph) gave large, nicely formed crystals, and one was subjected to an X-ray analysis. Unfortunately, the structure is badly disordered by exchange of the O and NHR group positions and could not be satisfactorily refined.

Deprotonation of both the NH and OH groups of **1** is not observed. Treatment of **1** with excess $LiN(SiMe_3)_2$ gives only the single deprotonation products **3**. With stronger bases ($LiNPr^i_2$, LiMe, and LiPh), reduction products (PtL_x) are detected (^{31}P NMR).

The L_2 = dppm derivatives are the only diamido complexes $[L_2Pt(\mu\text{-NHR})]_2(BF_4)_2$ (**2**) that were successfully deprotonated. However, like the hydroxo analogue, initial deprotonation occurs at the dppm ligand methylene group and not at the amido NH group. Treatment of THF suspensions of $[(dppm)Pt(\mu\text{-NHR})]_2(BF_4)_2$ (R = H, Ph, *p*-tol) with 2 equiv or more of $LiN(SiMe_3)_2$ yields a solution of the neutral dppm-H diamido complexes $[(dppm\text{-}H)Pt(\mu\text{-NHR})]_2$ (**4**) (R = H, Ph, *p*-tol, eq 4). Similar reactions occur with $NaN(SiMe_3)_2$ or $KN(SiMe_3)_2$.

$$[(dppm)Pt(\mu\text{-NHR})]_2(BF_4)_2 + 2LiN(SiMe_3)_2 \rightarrow \underset{\mathbf{4}}{} [(dppm\text{-}H)Pt(\mu\text{-NHR})]_2 + 2HN(SiMe_3)_2 + 2LiBF_4 \quad (4)$$

^{31}P NMR spectra of **4** show shifts in the expected region and a reduction in the P−Pt coupling constants from those of **2**. For the R = H derivative, a single peak with ^{195}Pt satellites is observed. The R = Ph and *p*-tol derivatives show two closely spaced peaks with similar P−Pt coupling constants. The peak ratios vary according to time and solvent and are assigned to two isomers (syn and anti, see Discussion). As prepared in THF, the ratios are ∼1:1. Freshly dissolved isolated samples in CD_2Cl_2 also show a ratio of ∼1:1, but as time passes the ratios

(26) O'Mahoney, C. A.; Parkin, I. P.; Williams, D. J.; Woollins, J. D. *Polyhedron* **1989**, *8*, 1979−1981.
(27) Park, S.; Rheingold, A. L.; Roundhill, D. M. *Organometallics* **1991**, *10*, 615−623.
(28) (a) Alcock, N. W.; Bergamini, P.; Kemp, T. J.; Pringle, P. G. *J. Chem. Soc., Chem. Commun.* **1987**, 235−236. (b) Alcock, N. W.; Bergamini, P.; Kemp, T. J.; Pringle, P. G. Sostero, S.; Traverso, O. *Inorg. Chem.* **1991**, *30*, 1594−1598.

Table 1. Crystallographic and Data Collection Parameters[a]

	1 (L = PPh_3, R = *p*-tol)	**4** (R = Ph)	**5**	**7**
formula	$C_{79}H_{71}NO_2P_4Pt_2(BF_4)_2 \cdot CH_2Cl_2$	$C_{62}H_{54}N_2P_4Pt_2$	$C_{58}H_{64}LiN_4O_2P_4Pt_2BF_4 \cdot 5(C_4H_8O)$	$C_{62}H_{58}N_2O_2P_4Pt_2 \cdot 2CH_2Cl_2$
fw	1820.96	1341.13	1817.46	1547.02
space group	$P2_1/n$ (No. 14)	$Pna2_1$ (No. 33)	$P2_1/n$ (No. 14)	$P2_1/n$ (No. 14)
T, °C	22	−100	−100	−100
a, Å	16.331(5)	38.272(2)	17.669(5)	10.5866(6)
b, Å	23.908(5)	9.2841(5)	31.884(3)	18.384(1)
c, Å	19.233(6)	15.0099(7)	14.686(4)	15.5680(8)
β, deg	99.01(1)		105.03(1)	94.34(1)
V, Å^3	7417(4)	5333.4(5)	7990(3)	3021.3(3)
Z	4	4	4	2
d_{calc}, g/cm^3	1.63	1.67	1.51	1.70
μ, mm^{-1}	3.99	5.40	3.64	4.95
transm range, %	0.899−1.00	0.729−1.00	0.754−0.998	0.827−1.00
R1,[b] wR2[c]	0.031, 0.060	0.052, 0.138	0.051, 0.070	0.021, 0.048

[a] λ = 0.71070 Å (Mo). [b] $R1 = (\sum||F_o| - |F_c||)/\sum|F_o|$. [c] $wR2 = [(\sum w(F_o^2 - F_c^2)^2)/\sum w(F_c^2)^2]^{1/2}$ with weight = $1/[\sigma^2(F_o^2) + (xP)^2 + yP]$; x = 0.0253, y = 0 for **1**, x = 0.282, y = 44.5 for **4**; x = 0.0925, y = 4.640 for **5**; x = 0.0238, y = 1.930 for **7**; $P = (F_o^2 + 2F_c^2)/3$.

Table 2. Distances and Angles for $[(L_2Pt)_2(\mu\text{-NHR})(\mu\text{-OH})](BF_4)_2 \cdot CH_2Cl_2$ (**1**·CH_2Cl_2) (L = PPh_3, R = *p*-tol)

Pt1−Pt2	3.159(1)	Pt1−N	2.101(6)
Pt2−P3	2.259(2)	N−HN	0.67(5)
Pt2−O	2.059(6)	Pt1−P2	2.237(2)
O−HO	0.62(7)	Pt1−O	2.066(6)
Pt1−P1	2.274(2)	Pt2−N	2.129(6)
Pt2−P4	2.232(2)	N−C1	1.434(9)
P1−Pt1−P2	96.91(6)	P3−Pt2−P4	96.95(7)
P1−Pt1−O	88.91(16)	P3−Pt2−O	93.47(17)
P2−Pt1−O	173.01(17)	P4−Pt2−O	169.52(17)
P1−Pt1−N	164.48(18)	P3−Pt2−N	168.75(18)
P2−Pt1−N	98.23(18)	P4−Pt2−N	94.28(18)
O−Pt1−N	75.8(2)	O−Pt2−N	75.3(2)
Pt1−O−Pt2	99.9(2)	Pt1−O−HO	126(8)
Pt2−O−HO	130(8)	Pt1−N−Pt2	96.6(2)
Pt1−N−C1	112.2(5)	Pt2−N−C1	117.6(5)
Pt1−N−HN	109(5)	Pt2−N−HN	111(5)
C1−N−HN	109(5)	N−C1−C2	119.8(6)
N−C1−C6	120.8(7)		

change until after 3 h the ratio remains stable at ∼1:2 (high-field peak largest for R = Ph, low-field peak largest for R = *p*-tol). In both cases, the most abundant isomer in CD_2Cl_2 has the largest Pt−P coupling constant.

^{1}H NMR spectra of the R = Ph and *p*-tol derivatives are consistent with the presence of isomers. The NHR groups appear as broad peaks between 2.4 and 3.1 ppm in the same ratios as the peaks observed in the ^{31}P NMR spectra. The signals for the dppm-H groups are sharp singlets between 3.2 and 3.4 ppm, again in the expected ratio. The dppm-H group signal for the R = H derivative is observed at 3.7 ppm, and with concentrated solutions, Pt satellites are detected (J_{PtH} = 188 Hz). Close examination of the ^{1}H NMR spectra of the Ph and *p*-tol derivatives suggests that the dppm-H peaks of these derivatives also have satellites, but the signals are too weak to confirm this. The NH_2 group of the R = H derivative is observed as a broad singlet at 0.2 ppm.

The deprotonation site is confirmed by a single-crystal structure analysis of **4** (R = Ph). A drawing of the structure is given in Figure 2. The deprotonation of the dppm group is evident from the short P−C distances (1.72 Å average) and the presence of a single carbon bonded hydrogen atom located in the P−C−P plane. An abbreviated summary of crystal data and data collection and processing is given in Table 1. Selected bond distances and angles are listed in Table 3.

A similar deprotonation occurs for the dihydrazido complex **2** (L_2 = dppm, R = NH_2). Again, spectroscopic data indicate deprotonation of the dppm ligand. However, IR spectra also

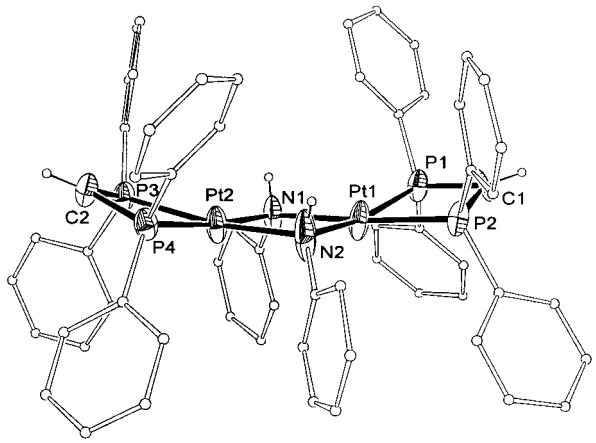

Figure 2. ORTEP drawing of $[(dppm\text{-}H)Pt(\mu\text{-}NHPh)]_2$ (**4**) (R = Ph).

Table 3. Distances and Angles for $[(dppm\text{-}H)Pt(\mu\text{-}NHPh)]_2$ (**4**) (R = Ph)

Pt1−Pt2	3.2102(6)	P2−C1	1.718(13)
Pt1−N2	2.104(15)	N1−C3	1.34(2)
Pt2−N1	2.166(10)	Pt1−P2	2.258(3)
P1−C1	1.728(10)	Pt2−N2	2.108(11)
P4−C2	1.734(11)	Pt2−P4	2.257(4)
Pt1−P1	2.232(4)	P3−C2	1.712(13)
Pt1−N1	2.142(9)	N2−C9	1.50(2)
Pt2−P3	2.250(3)		
P1−Pt1−P2	70.55(12)	N2−Pt1−N1	82.4(4)
N2−Pt1−P1	166.1(5)	N1−Pt1−P1	102.8(3)
N2−Pt1−P2	103.5(3)	N1−Pt1−P2	173.1(3)
P3−Pt2−P4	70.37(12)	N2−Pt2−N1	81.7(5)
N2−Pt2−P3	168.2(5)	N1−Pt2−P3	103.8(3)
N2−Pt2−P4	103.1(4)	N1−Pt2−P4	172.5(3)
C3−N1−Pt1	121.4(9)	C3−N1−Pt2	116.3(9)
Pt1−N1−Pt2	96.4(4)	C9−N2−Pt1	120.2(10)
C9−N2−Pt2	116.4(9)	Pt1−N2−Pt2	99.3(6)
P2−C1−P1	97.6(6)	P3−C2−P4	97.8(6)

show the presence of a BF_4 ion. The reason for this is apparent from the structure of the product **5** as determined by X-ray crystallography. A drawing of the structure is shown in Figure 3. An abbreviated summary of crystal data and data collection and processing is given in Table 1. Selected bond distances and angles are listed in Table 4. The structure of the cationic portion shows the expected edge-shared square-planar Pt centers folded at the edge with bridging $NHNH_2$ groups and deprotonated dppm ligands. The $NHNH_2$ groups bridge the two Pt atoms through the NH portion. The NH_2 portions coordinate to a $Li(THF)_2^+$ group in a "tweezers" fashion resulting in tetrahedral

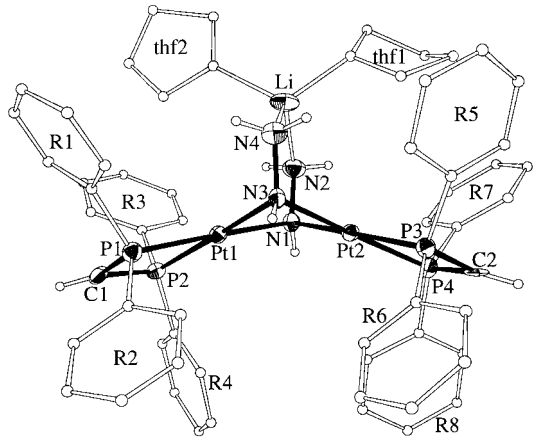

Figure 3. ORTEP drawing of the cationic portion of [{(dppm-H)Pt(μ-NHNH$_2$)}$_2$Li(THF)$_2$](BF$_4$) (**5**).

Table 4. Selected Distances and Angles for [(dppm-H)Pt(μ-NHNH$_2$)]$_2$[Li(THF)$_2$](BF$_4$) (**5**)

Pt1−Pt2	3.0718(9)	P2−C1	1.716(11)
Pt2−P3	2.251(3)	O1−Li	1.88(2)
Pt1−N3	2.104(10)	N3−N4	1.461(13)
P1−C1	1.704(12)	Pt1−P2	2.256(3)
P4−C2	1.702(11)	Pt1−N1	2.092(8)
N1−N2	1.472(13)	Pt2−N3	2.075(9)
N4−Li	2.06(2)	P3−C2	1.709(12)
Pt1−P1	2.248(3)	O2−Li	1.94(2)
Pt2−P4	2.254(3)	N2−Li	2.06(2)
Pt2−N1	2.094(9)		
P1−Pt1−P2	70.30(11)	N1−Pt1−N3	77.1(4)
P3−Pt2−P4	69.98(11)	N3−Pt2−N1	77.7(4)
N1−Pt1−P1	176.4(3)	N3−Pt1−P2	176.6(3)
N1−Pt2−P3	175.9(2)	N3−Pt2−P4	176.4(3)
N3−Pt1−P1	106.4(3)	N1−Pt1−P2	106.2(3)
N3−Pt2−P3	106.4(3)	N1−Pt2−P4	105.9(2)
N2−N1−Pt1	113.7(6)	N2−N1−Pt2	112.0(6)
Pt1−N1−Pt2	94.4(3)	N1−N2−Li	114.5(9)
N4−N3−Pt2	115.7(7)	N4−N3−Pt1	112.9(6)
Pt2−N3−Pt1	94.6(4)	N3−N4−Li	112.8(9)
P1−C1−P2	98.6(6)	P4−C2−P3	98.5(6)
O1−Li−O2	116.0(11)	O1−Li−N4	109.1(11)
O2−Li−N4	107.7(12)	O1−Li−N2	109.7(12)
O2−Li−N2	107.7(11)	N4−Li−N2	106.1(10)

coordination about the Li ion. The deprotonation of **2** (L_2 = dppm, R = NH_2) is therefore described by eq 5.

$$[(\text{dppm})\text{Pt}(\mu\text{-NHNH}_2)]_2(\text{BF}_4)_2 + 2\text{LiN(SiMe}_3)_2 + 2\text{THF} \rightarrow \underset{\mathbf{5}}{[\{(\text{dppm-H})\text{Pt}(\mu\text{-NHNH}_2)\}_2\text{Li(THF)}_2]\text{BF}_4} + 2\text{HN(SiMe}_3)_2 + \text{LiBF}_4 \quad (5)$$

Complexes **4** (but not **5**) can be further deprotonated with stronger bases. Treatment of **4** with 2 equiv of LiMe produces, after workup, Li$_2$[(dppm-H)Pt(μ-NR)]$_2$ (**6**) (R = H, Ph, *p*-tol; eq 6).[29] These products are very sensitive and, with the exception of THF, are insoluble in all solvents with which they do not react. ^{31}P NMR spectra in THF show a single peak with satellites in the −40 to −50 ppm range, indicating retention of the chelating phosphine. Consistent with the generation of a strong donor ligand trans to the phosphine, the Pt−P coupling constants are decreased from those of **4**. IR data show a single NH peak at 3361 cm^{-1} for R = H and no NH peaks for R = Ph and *p*-tol, indicating conversion of the NHR groups to NR groups.

$$\underset{\mathbf{4}}{[(\text{dppm-H})\text{Pt}(\mu\text{-NHR})]_2} + 2\text{LiMe} \rightarrow \underset{\mathbf{6}\ (\text{R} = \text{H, Ph, } p\text{-tol})}{\text{Li}_2[(\text{dppm-H})\text{Pt}(\mu\text{-NR})]_2} + 2\text{MeH} \quad (6)$$

Complex **6** (R = Ph) produces beautiful yellow crystals from cold THF solutions. These crystals dissolve rapidly on warming and are very sensitive to desolvation and to decomposition from air exposure. Low-temperature X-ray diffraction data sets were successfully collected at several different temperatures on several different crystals. None of the resulting structures refined well, but the results are consistent with the structural formula [{(dppm-H)Pt(μ-NPh)}$_2$Li(THF)$_2$][Li(THF)$_4$]·THF. This chemically reasonable structure is compatible with the structures of the related oxo complexes [(dppm-H)Pt(μ-OLi(THF)$_2$)]$_2$ and [{(PPh$_3$)$_2$Pt(μ-O)}$_2$LiBF$_4$][17] and with the structure of the analogous imido complex [(pnp)Pt{μ-N(2,6-Me$_2$C$_6$H$_3$)}]$_2$LiNO$_3$ (pnp = Ph$_2$PN(Me)PPh$_2$).[30] Elemental analysis results on desolvated crystals of **6** (R = Ph) match the formulation [(dppm-H)Pt(μ-NPh)]$_2$Li$_2$.

Exposure of solutions of **6** to air gives purple solutions. A yellow crystal obtained from one of these solutions was subjected to X-ray analysis. The structure was revealed to be [(PMePh$_2$)(OPPh$_2$)Pt(μ-NHPh)]$_2$ (**7**). This complex is likely formed by base-induced cleavage of the dppm P−CH$_2$−P unit as was previously observed in the reaction of (dppm)PtCl$_2$ with NaOH and ammonia.[28,31] A drawing of the structure is given in Figure 4. An abbreviated summary of crystal data and data collection and processing is supplied in Table 1. Selected bond distances and angles are listed in Table 5.

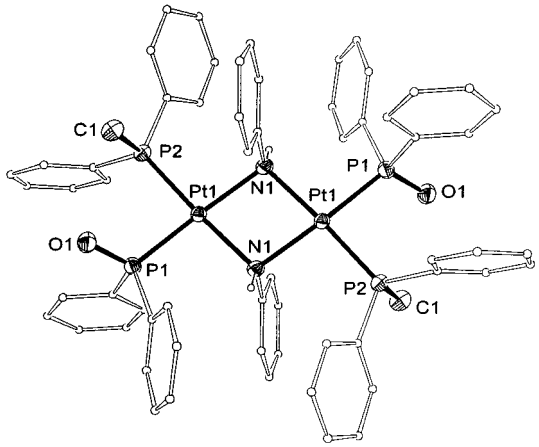

Figure 4. ORTEP drawing of [(OPPh$_2$)(MePPh$_2$)Pt(μ-NHPh)]$_2$ (**7**).

Table 5. Selected Distances and Angles for [(PMe$_2$Ph)(OPMe$_2$)Pt(μ-NPh)]$_2$ (**7**)

Pt1−N1	2.126(2)	P1−O1	1.509(2)
Pt1−P1	2.2530(7)	Pt1−P2	2.2514(7)
Pt1−N1	2.176(2)	N1−C11	1.433(3)
N1−Pt1−N1	79.55(10)	N1−Pt1−P2	176.46(7)
N1−Pt1−P2	96.93(6)	N1−Pt1−P1	96.65(7)
N1−Pt1−P1	167.04(6)	C11−N1−Pt1	116.12(16)
C11−N1−Pt1	107.22(17)	Pt1−N1−Pt1	100.45(10)

(29) The related Ir diimido complex Li$_2$[(CO)$_2$Ir(μ-NR)]$_2$ has been prepared by a similar deprotonation reaction: Kolel-Veetil, M. K.; Ahmed, K. J. *Inorg. Chem.* **1994**, *33*, 4945−4949.

(30) Holbert, T.; Sharp, P. To be published.

(31) See also: Lin, I. J. B.; Lai, J. S.; Liu, C. W. *Organometallics* **1990**, *9*, 530−531.

Discussion

Amido Complexes. Aminolysis reactions of late transition metal hydroxo complexes have been reported previously. Nutton and Maitlis described the synthesis of $[(Cp^*M)_2(\mu\text{-}OH)_2(NHPh)]^+$ by aniline addition to an aqueous solution of $[(Cp^*M)_2(\mu\text{-}OH)_3]^+$ (M = Rh, Ir).[24] Similarly, Lopez and coworker converted $[Pd(C_6F_5)(PPh_3)(\mu\text{-}OH)]_2$ to $\{Pd(C_6F_5)(PPh_3)\}_2(\mu\text{-}OH)(NHC_6H_5X\text{-}p)$ with $NH_2C_6H_5X\text{-}p$.[23] More recently, Driver and Hartwig obtained $\{Pd(Ph)(PPh_3)\}_2(\mu\text{-}OH)(NHR)$ (R = Bu^t, Bu^s, 2,6-$Me_2C_6H_3$) from the reaction of $[Pd(Ph)(PPh_3)(\mu\text{-}OH)]_2$ with NH_2R.[16,25] In all these cases, addition of excess amine did not give further substitution of the hydroxo group. For the $Pd(C_6F_5)$ complexes, kinetic inhibition was postulated presumably as a result of steric crowding. The successful conversion of in situ generated mixtures of $[Pd(C_6F_5)(CNBu^t)(\mu\text{-}OH)]_2$ and $[Pd(C_6F_5)(CNBu^t)(\mu\text{-}OMe)]_2$ to the diamido analogue is consistent with reduced steric inhibition,[23] as is the observation by Driver and Hartwig that the formation of the diamido, $[Pd(C_6F_5)(PPh_3)(\mu\text{-}NHBu^i)]_2$, is possible in the reaction of $[Pd(Ph)(PPh_3)(\mu\text{-}OH)]_2$ with the less sterically demanding amine NH_2Bu^i.[16,25]

Steric inhibition is probably also involved in the aminolysis reactions studied here. This is suggested by the observation that the PPh_3 and the dppp dihydroxo complexes give only the amido−hydroxo complexes $[(L_2Pt)_2(\mu\text{-}NHR)(\mu\text{-}OH)](BF_4)_2$ (**1**) in their reactions with aryl amines whereas the other phosphine hydroxo complexes give complete reaction to the diamido complexes $[L_2Pt(\mu\text{-}NHR)]_2(BF_4)_2$ (**2**). With the sterically less demanding amine NH_3, the dppp dihydroxo complex also gives complete exchange, producing the diamido complex **2**. Although we did not attempt it, the PPh_3 complex probably would as well.[32] These results may be rationalized if it is realized that replacement of the first OH with an aryl amido group results in a more crowded complex. The failure of the PPh_3 complexes to progress further is possibly due to the greater steric demand of PPh_3 over PMe_2Ph and the chelating ligands. The propylene bridge of the dppp ligand may fold up from the P_2Pt plane orienting the phenyl rings in a way to hinder access to the Pt centers. With ammonia, sterics would not be an issue since an NH_2 group is sterically comparable to an OH group.

Other methods have been used to prepare dinuclear Pt amido complexes including some of the same NH_2 derivatives prepared here. $[L_2Pt(\mu\text{-}NH_2)]_2(BF_4)_2$ (**2**) (R = H, L_2 = dppe, L = PMe_3, PMe_2Ph, $PMePh_2$, PEt_3) were isolated from the reaction of L_2PtCl_2 with mixtures of HBF_4 and Na in liquid ammonia.[26] Neutral $[LPtX(\mu\text{-}NH_2)]_2$ (L = PPh_3, PEt_3, PCy_3, $PMePh_2$, X = H, Me) were obtained from $[L_2PtX(NH_3)]^+$ and $NaNH_2$.[27] The L = $PMePh_2$, X = $OPPh_2$ derivative was isolated from the reaction of $(dppm)PtCl_2$ with NaOH and ammonia.[28] Related dinuclear Pt amido complexes where the amido group is part of a chelating ligand have also been reported.[33] Pd dinuclear amido complexes are also known and include aryl derivatives.[34,35] Methods for the preparation of these complexes include deprotonation of monomeric amine complexes, reaction of iodide complexes with LiNHR, and aminolysis reactions of hydroxo complexes, monomeric methyl complexes, and acac complexes.

Deprotonation Reactions. The amido−hydroxo complexes $[(L_2Pt)_2(\mu\text{-}NHR)(\mu\text{-}OH)](BF_4)_2$ (**1**) provide useful test complexes for the relative acidity of the hydroxo and amido groups (or conversely, the basicity of the oxo and imido groups). The hydroxo group is evidently the most acidic, and it is the group that is deprotonated first. This is consistent with the higher acidity of water and alcohols over amines. This also agrees with previous observations on deprotonations of the A-frame complexes $[M_2(\mu\text{-}Y)(CO)_2(\mu\text{-}dppm)_2]^+$ (M = Rh, Ir; Y = OH, NHR), where the properties of the complexes and their deprotonation products indicate that the amido group is the less acidic.[36] In contrast to the A-frame complexes where the aryl amido group is deprotonated by $LiN(SiMe_3)_2$, amido group deprotonation is not observed for the amido−oxo complexes $[(L_2Pt)_2(\mu\text{-}NHR)(\mu\text{-}O)](BF_4)$ (**3**). Our failure to deprotonate the amido groups with $LiN(SiMe_3)_2$ suggests that the amido groups in these complexes have a lower acidity than those of the A-frame complexes.[37] Stronger bases do not deprotonate but reduce the Pt centers, indicating that reaction pathways other than deprotonation have become dominant.

Consistent with the low acidity of the amido−oxo complexes **3**, most of the diamido complexes **2** are not deprotonated. The dppm derivatives, $[(dppm)Pt(\mu\text{-}NHR)]_2(BF_4)_2$ (**2**) (L_2 = dppm), are exceptional in that they do deprotonate although dppm ligand deprotonation precedes amido group deprotonation. This is analogous to the hydroxo system where $[(dppm)Pt(\mu\text{-}OH)]_2(BF_4)_2$ is deprotonated first at the dppm ligand.[17] The unique deprotonation of the dppm diamido complexes might indicate that the dppm ligand imparts greater acidity to the amido ligands.[38] The dppm complexes, including the hydroxo complex, do show unique P−Pt coupling constants. The coupling constants are consistently lower for the dppm complexes by 143−420 Hz. Lower coupling constants are related to decreasing amounts of Pt s-character in the P−Pt bonds.[22] Decreased s-character is expected as a result of the acute P−Pt−P bond angle induced by the small "bite angle" of the dppm and dppm-H ligands and should result in greater s-character in the Pt−N bonds. The greater Pt s-character in the Pt−N bonds results in more electron density transfer from N to Pt and more acidic amido groups. IR and ^{1}H NMR data are ambiguous in this regard.[39] The average $\sqrt{}$(NH) IR bands are nearly identical (within 12 cm^{-1}) for the series of complexes containing the dppm, dppe, and dppp ligands. ^{1}H NMR data do show that the dppm complexes have a lower field NH shift (1.9−2.7 ppm lower) for the R = Ph, *p*-tol, and NH_2 complexes as compared to the dppe analogues but for the R = H series the shifts are essentially identical for all phosphine ligands.

An alternative or additional explanation is that the dppm or dppm-H ligand stabilizes the complexes to reduction and reactions other than deprotonation. The second deprotonation of the dppm complexes with LiMe to give the anionic imido

(32) (a) $[L_2Pt(\mu\text{-}NH_2)]_2(BF_4)_2$ (L = PPh_3) is believed to have formed in the reaction of hydrazine with L_2PtCl_2: Dobson, G. C.; Mason, R.; Robertson, G. B.; Conti, D.; R. U. F.; Morelli, D.; Cenini, S.; Bonati, F. *J. Chem. Soc., Chem. Commun.* **1967**, 739. (b) The formation of $[L_2Pt(\mu\text{-}NH_2)]_2(BF_4)_2$ (L = PPh_3, PPh_2Me) from the reaction of the hydroxo analogues with NH_3(aq) is described in ref 28b.

(33) Freeman, W. A.; Nicholls, L. J.; Liu, C. F. *Inorg. Chem.* **1978**, *17*, 2989−2994. Cooper, M. K.; Stevens, P. V.; McPartlin, M. *J. Chem. Soc., Dalton Trans.* **1983**, 553.

(34) Okeya, S.; Yoshimatsu, H.; Nakamura, Y.; Kawaguchi, S. *Bull. Chem. Soc. Jpn.* **1982**, *55*, 483−491.

(35) Villanueva, L. A.; Abboud, K. A.; Boncella, J. A. *Organometallics* **1994**, *13*, 3921−3931.

(36) (a) Sharp, P. R.; Flynn, J. R. *Inorg. Chem.* **1987**, *26*, 3231−3234. (b) Ge, Y.-W.; Peng, F.; Sharp, P. R. *J. Am. Chem. Soc.* **1990**, *112*, 2632−2640. (c) Ye, C.; Sharp, P. R. *Inorg. Chem.* **1995**, *34*, 55−59.

(37) Solubility differences between the protonated and deprotonated forms of the complexes complicate acidity comparisons.[17]

(38) Hofmann has noted unique features of the chemistry of Pt complexes with small bite angle phosphine ligands: Hofmann, P. In *Organometallics in Organic Synthesis*; de Meijiere, A., tom Dieck, H., Eds.; Springer: Berlin, 1987; p 1 and references cited therein.

(39) Anomalous IR and ^{1}H NMR data were noted previously for the dppm hydroxo complex.[17]

complexes $Li_2[(dppm\text{-}H)Pt(\mu\text{-}NR)]_2$ (**6**) is certainly remarkable and is in marked contrast to the reduction observed for the PPh_3 amido−oxo complexes **3** when these were treated with LiMe or other strong bases. Stability to reduction could result from the small "bite angle" of the chelating dppm and dppm-H ligands, which is incompatible with the geometries (linear, trigonal planar, or tetrahedral) of Pt(0) complexes.

Structures. A comparison of the metrical parameters of $[(L_2Pt)_2(\mu\text{-}NHR)(\mu\text{-}OH)](BF_4)_2$ (**1**) (L = PPh_3, R = *p*-tol, Figure 1) with the previously reported hydroxo analogue $[(PPh_3)_2Pt(\mu\text{-}OH)_2](BF_4)_2$ shows few changes.[17] The major difference is the fold along the common edge of the two Pt square-planar coordination spheres of **1**. The hydroxo complex is planar. Despite this difference the Pt−O distances (2.066 Å average) of **1** are essentially identical to those of the hydroxo complex (2.063 Å average), as is the Pt−Pt distance (3.159 Å versus 3.153 Å). The Pt−P distances are slightly longer (2.251 Å average versus 2.220 Å average) most likely as a result of the stronger donor strength of the amido group. The Pt−P distances (2.250 Å) in $[(PMe_2Ph)Pt(\mu\text{-}NH_2)]_2(BF_4)_2$ are similar.[26] An internal comparison of the Pt−N and Pt−O distances in **1** shows that the Pt−N distances (2.122 Å average) are 0.056 Å longer than the Pt−O distances, close to the 0.04 Å difference between the covalent radius of O and N.[40] The Pt−N distances of **1** are however, slightly longer than the 2.086 Å Pt−N distances in $[(PMe_2Ph)Pt(\mu\text{-}NH_2)]_2(BF_4)_2$.

A curious feature of the structure of $[(dppm\text{-}H)Pt(\mu\text{-}NHR)]_2$ (**4**) (R = Ph) is the apparent inequivalence of the Pt−N distances for the two amido groups. Although the errors are large, the Pt distances to N2 (2.104(15) and 2.108(11) Å) appear shorter than those to N1 (2.142(9) and 2.166(10) Å). Along with the longer Pt−N1 distances is a shorter N−phenyl ring carbon distance (N1−C =1.34(2) Å, N2−C = 1.50(2) Å). We have previously attributed short N−C distances in imido complexes to delocalization of nitrogen atom electron density into the aryl ring.[36] A similar interpretation here would indicate a contribution of resonance form **B** to the bonding of the N1 amido group to the Pt centers. However, it is not clear why only one of the amido ligands would display this feature. Given the difficulties (disorder, unreasonable structures, etc.) that we have encountered with many of the X-ray structures in these dimeric systems and the large errors in the metrical parameters of this structure, the inequivalence of the Pt−N distances may be deceptive.

B

The structure of $[(dppm\text{-}H)Pt(\mu\text{-}NHR)]_2$ (**4**) (R = Ph) and the cationic portion of $[\{(dppm\text{-}H)Pt(\mu\text{-}NHNH_2)\}_2Li(THF)_2]BF_4$ (**5**) share some features with that of **1**. However, with the deprotonated dppm ligands of **4** and **5** detailed comparisons are perhaps better made with the deprotonated oxo complex, $Li_2[(dppm\text{-}H)Pt(\mu\text{-}O)]_2$, which crystallizes as $[(dppm\text{-}H)Pt(\mu\text{-}O)]_2[Li(THF)_2]_2$.[17] The Pt−N distances of **4** average to 2.13 Å, and those of **5** average to 2.09 Å. The value for **5** compares favorably with the average Pt−O distance of 2.05 Å observed for the dioxo complex and matches the 0.04 Å difference in O and N covalent radii.[40] The hydrazido and amido complexes show longer average P−Pt distances (2.252 and 2.249 Å vs 2.223 Å). The angles around the Pt atoms are almost identical in all three complexes despite the folded nature of **4** and **5** and the planar geometry of the oxo complex. The N−N distance of 1.44 Å in **5** is consistent with the expected single bond and compares favorably with other hydrazido structures.[41] The bonding of the Li ion should be weaker for the neutral hydrazido complex than for the anionic dppm-H oxo complex and this is reflected in the much longer average N−Li distances (2.06 Å) of **5** versus the O−Li distance (1.76(2) Å) of the oxo complex.

Many of the dinuclear complexes studied here have the possibility of isomers based on the orientation of the hydrogen atoms and the R groups on the oxygen and nitrogen bridging atoms. More are possible for the folded than for the planar structures.[42] However, since the energy difference between the folded and planar structures is believed to be small,[43] a static folded structure is unlikely in solution, and isomers derived from a static folded geometry may be neglected. For planar dimers or rapidly "flopping" folded dimers, isomers due to "syn" (**S**) or "anti" (**A**) orientations of the groups on the bridging atoms are possible for the amido−hydroxo (assuming a nonplanar oxygen atom), the diamido, and the diimido complexes (assuming a nonplanar nitrogen atom). Such isomers have been observed in solution with some related systems[25,34,35,44] but not with others.[45] Solution NMR data show evidence for isomers only for **4** (R = Ph, *p*-tol). Evidently, for the other complexes either one isomer is dominant or, if more than one is present, exchange is rapid.

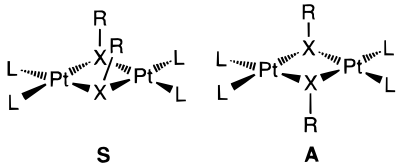

Conclusions

The conversion of dimeric dihydroxo complexes to the analogous amido−hydroxo and diamido complexes has been achieved by aminolysis reactions. The extent of the amido for hydroxo substitution is apparently controlled by steric factors. Deprotonation reactions of the amido−hydroxo complexes show that the hydroxo group is the more acidic, consistent with earlier observations on other late transition metal systems. Deprotonation of the amido group is only observed in the dppm diamido complexes and then only after the dppm methylene group is deprotonated. Why the dppm-H ligand is unique in allowing deprotonation of the amido group to an imido group is uncertain but is probably related to the small bite angle of the dppm-H ligand and the resulting hybridization at the Pt centers.

Experimental Section

General Procedures. Experiments were performed under a dinitrogen atmosphere in a Vacuum Atmospheres Corporation drybox or by Schlenk techniques unless otherwise indicated. Solvents were dried

(40) Jolly, *W. L. Modern Inorganic Chemistry*, 2nd ed.; McGraw Hill: New York, 1991.

(41) (a) Heaton, B. T. *Coord. Chem. Rev.* **1996**, *154*, 193−229. (b) Hidai, M.; Mizobe, Y. *Chem. Rev.* **1995**, *95*, 1115−1133. (c) Sutton, D. *Chem. Rev.* **1993**, *93*, 995−1022.

(42) For recent theoretical work on the determining factors in the molecular conformation of d^8 dimers, see: Aullon, G.; Ujaque, G.; Lledos, A.; Alvarez, S.; Alemany, P. *Inorg. Chem.* **1998**, *37*, 804−813.

(43) Theoretical studies indicate small energy differences between the folded and planar structures: Summerville, R. H.; Hoffmann, R. *J. Am. Chem. Soc.* **1976**, *98*, 7240.

(44) Brunet, J.-J.; Commenges, G.; Neibecker, D.; Philippot, K.; Rosenberg, L. *Inorg. Chem.* **1994**, *33*, 6373−6379.

(45) Kolel-Veetil, M. K.; Rahim, M.; Edwards, A. J.; Rheingold, A. L.; Ahmed, K. J. *Inorg. Chem.* **1992**, *31*, 3877−3878. Kolel-Veetil, M. K.; Rheingold, A. L.; Ahmed, K. J. *Organometallics* **1993**, *12*, 3439−3446.

by standard techniques and were stored under dinitrogen over 4 Å molecular sieves. CP grade gases were purchased from Matheson and used as received. Silver tetrafluoroborate, silver triflate, $LiN(SiMe_3)_2$, $LiNPr^i_2$, LiMe (1.4 M in ether), and amines were purchased from Aldrich Chemicals and, with the exception of the following, were used as received. Aniline and 4-*tert*-butylaniline (Aldrich) were distilled and $LiN(SiMe_3)_2$ and $LiNPr^i_2$ were recrystallized prior to use. $[L_2Pt(\mu\text{-}OH)_2]_2(BF_2)_2$ (L = PPh_3,[18c] PMe_2Ph,[17] L_2 = dppe,[19,46] dppm,[17,19] dppp,[17,19] dppb[17,19]) and $[(Ph_3P)_2Pt(OH_2)_2](OTf)_2$[47] were synthesized according to literature procedures. NMR spectra were recorded on JEOL FX 90Q, Nicolet NT-300WB, or Bruker AMX-500 or AMX-250 spectrometers. ^{1}H NMR spectra are referenced to TMS or to protic solvent impurities referenced back to TMS. ^{31}P NMR spectra were referenced to external 85% H_3PO_4. All NMR shifts are in parts per million with negative shifts upfield from the reference. Infrared spectra were recorded on a Nicolet 20 DXB FTIR spectrometer using NaCl plates and are given in wavenumbers (cm^{-1}). Spectra were recorded at ambient temperatures unless otherwise indicated. Microanalyses (inert atmosphere) were performed by Desert Analytics or Oneida Research Services, Inc.

Amido−Hydroxo Complexes $[(L_2Pt)_2(\mu\text{-}OH)(\mu\text{-}NHR)](BF_4)_2$ 1. L = PPh_3, R = Ph. A 250 mL flask was charged with $[(PPh_3)_2Pt(\mu\text{-}OH)]_2(BF_4)_2$ (500 mg, 0.304 mmol), 200 mL of CH_2Cl_2 and a stir bar. A homogeneous pale-orange solution resulted upon aniline (1.00 mL, 11.0 mmol) addition. The reaction mixture was stirred for 2 h and concentrated to 100 mL, and 200 mL of ether was added. The resulting off-white solid was recovered by filtration, washed with ether, and dried in vacuo. Recrystallization was achieved by dissolving the product in a minimum amount of CH_2Cl_2, adding an equal amount of ether, and cooling the mixture at 0 °C overnight. The white crystalline material was recovered by filtration, washed with ether, and dried in vacuo. Yield: 470 mg (91%). IR (mineral oil): 3543 (m, $\surd_{OH}$), 3288 (m, $\surd_{NH}$). ^{1}H NMR (500 MHz, $CDCl_3$): 2.45 (s, 1H, NH or OH), −1.03 (s, 1H, NH or OH). ^{31}P{^{1}H} NMR (121 MHz, CH_2Cl_2): 9.83 (d, J_{P-P} = 20 Hz, J_{P-Pt} = 3064 Hz, P trans to N), 2.66 (d, J_{P-Pt} = 3910 Hz, P trans to O).

L = PPh_3, R = *p*-tol. A 20 mL vial was charged with $[(PPh_3)_2Pt(\mu\text{-}OH)]_2(BF_4)_2$ (500 mg, 0.304 mmol) and *p*-toluidine (1.0 g, 9.3 mmol). The mixture was heated and stirred at 70 °C for 5 h. The white $[(PPh_3)_2Pt(\mu\text{-}OH)]_2(BF_4)_2$ dissolved in the molten toluidine, and an orange homogeneous solution resulted. The hot solution was quickly transferred to a 200 mL beaker, and 100 mL of ether was added. The resulting pale-yellow solid was collected by filtration, washed with ether, and dried in vacuo. Recrystallization from CH_2Cl_2−ether yielded the pure product as a white solid. Yield: 460 mg (87%). Anal. Calcd (found) for $C_{79}H_{69}B_2F_8NOP_4Pt_2{\cdot}CH_2Cl_2$: C, 52.77 (53.10); H, 3.93 (3.90); N, 0.77 (0.72). The presence of CH_2Cl_2 was confirmed by ^{1}H NMR spectroscopy. IR (mineral oil): 3555 (m, $\surd_{OH}$), 3294 (m, $\surd_{NH}$). ^{1}H NMR (500 MHz, $CDCl_3$): 2.41 (s, 3H, CH_3), 2.15 (s, 1H, NH or OH), −0.95 (s, 1H, NH or OH). ^{31}P{^{1}H} NMR (121 MHz, CH_2Cl_2): 10.3 (d, J_{P-P} = 20 Hz, J_{P-Pt} = 3061 Hz, P trans to N), 3.0 (d, J_{P-Pt} = 3915 Hz, P trans to O).

L = PPh_3, R = *p*-Bu^{t}C$_6$H$_4$. A procedure analogous to that given for R = Ph gave the product as a white solid. Yield: 465 mg (86%). Anal. Calcd (found) for $C_{82}H_{75}B_2F_8NOP_4Pt_2$: C, 55.39 (55.60); H, 4.25 (4.22); N, 0.79 (0.83). IR (mineral oil): 3551 (m, $\surd_{OH}$), 3290 (m, $\surd_{NH}$). ^{1}H NMR (500 MHz, $CDCl_3$): 2.54 (s, 1H, NH or OH), 1.35 (s, 9H, CH_3), −1.04 (s, 1H, NH or OH). ^{31}P{^{1}H} NMR (121 MHz, CH_2Cl_2): 10.5 (d, J_{P-P} = 20 Hz, J_{P-Pt} = 3056 Hz, P trans to N), 3.1 (d, J_{P-Pt} = 3934 Hz, P trans to O).

L = PPh_3, R = *p*-NO$_2$C$_6$H$_4$. A solution of *p*-nitroaniline (1.00 g, 7.24 mmol) in CH_2Cl_2 (100 mL) was added to a stirred solution of $[(PPh_3)_2Pt(\mu\text{-}OH)]_2(BF_4)_2$ (1.00 g, 0.607 mmol) in CH_2Cl_2 (200 mL). The reaction mixture was stirred for 5 h and concentrated to 100 mL, and 200 mL of ether was added. The resulting pale-yellow solid was recovered by filtration, washed with toluene and then ether, and dried in vacuo. Recrystallization from CH_2Cl_2−ether yielded the product as a pale-yellow solid. Yield: 950 mg (88%). IR (mineral oil): 3549 (m, $\surd_{OH}$), 3287 (m, $\surd_{NH}$). ^{1}H NMR (500 MHz, $CDCl_3$): 2.84 (s, 1H, NH or OH), −1.10 (s, 1H, NH or OH). ^{31}P{^{1}H} NMR (121 MHz, CH_2Cl_2): 9.45 (d, J_{P-P} = 20 Hz, J_{P-Pt} = 3200 Hz, P trans to N), 3.49 (d, J_{P-Pt} = 3854 Hz, P trans to O).

A similar procedure using $[(PPh_3)_2Pt(H_2O)_2](OTf)_2$ gave pale-yellow $[(PPh_3)_4Pt_2(\mu\text{-}OH)(\mu\text{-}NHR)](OTf)_2$ (R = *p*-$NO_2C_6H_4$) (**1a**), the triflate analogue of **1** (L = PPh_3, R = *p*-$NO_2C_6H_4$), in the same yield. This sample was used for analysis. Spectroscopic data were essentially identical to those for the BF_4 analogue. Anal. Calcd (found) for $C_{79}H_{66}F_6N_2O_9P_4S_2Pt_2$: C, 50.48 (50.14); H, 3.54 (3.39); N, 1.49 (0.80).

L_2 = dppp, R = Ph. Aniline (0.037 g, 0.40 mmol) was added to a suspension of $[(dppp)Pt(\mu\text{-}OH)]_2(BF_4)_2$ (284 mg, 0.200 mmol) in THF (10 mL). The reaction mixture was refluxed under nitrogen for 40 min and then cooled to room temperature. The resulting off-white product was recovered by filtration, washed with THF, and dried at 80 °C in vacuo for 24 h. Yield: 255 mg (86%). IR (mineral oil): 3560 (m, $\surd_{OH}$), 3233 (m, $\surd_{NH}$). ^{1}H NMR (250 MHz, DMSO-d_6): 7.2−7.9 (40H, PPh), 6.5−7.0 (5H, NPh), 5.9 (br s, 1H, NH or OH), 5.0 (br s, 1H, NH or OH), 2.8 (br m, 8H, $PCH_2CH_2CH_2P$), 1.8 (br m, 4H, $PCH_2CH_2CH_2P$). ^{31}P{^{1}H} NMR (121 MHz, THF): −5.4 (d, J_{P-P} = 28 Hz, J_{P-Pt} = 2840 Hz, P trans to N), −9.5 (d, J_{P-Pt} = 3470 Hz, P trans to O).

L_2 = dppp, R = *p*-tol. A procedure analogous to that given for R = Ph gave the product as an off-white solid. Yield: 82%. Anal. Calcd (found) for $C_{54}H_{58}NP_4Pt_2B_2F_8O$: C, 44.22 (44.53); H, 3.99 (3.99); N, 3.82 (3.71). IR (mineral oil): 3563 (m, $\surd_{OH}$), 3234 (m, $\surd_{NH}$). ^{1}H NMR (250 MHz, DMSO-d_6): 7.3−7.9 (40H, PPh), 6.5−6.9 (4H, NPh), 5.9 (br s, 1H, NH or OH), 5.0 (br s, 1H, NH or OH), 2.7 (br m, 8H, $PCH_2CH_2CH_2P$), 2.0 (br m, 4H, $PCH_2CH_2CH_2P$), 1.70 (s, 3H, CH_3). ^{31}P-{^{1}H} NMR (121 MHz, DMSO): −5.2 (d, J_{P-P} = 28 Hz, J_{P-Pt} = 2834 Hz, P trans to N), −9.7 (d, J_{P-Pt} = 3472 Hz, P trans to O).

Diamido Complexes $[L_2Pt(\mu\text{-}NHR)]_2(BF_4)_2$ (2). L_2 = dppm, R = H. NH_3 gas was bubbled slowly through a stirred suspension of $[(dppm)Pt(\mu\text{-}OH)]_2(BF_4)_2$ (342 mg, 0.250 mmol) in THF (10 mL). The gas flow was stopped after 2 min, and the mixture was stirred for another 20 min. The white product was recovered by filtration, washed with THF, and dried in vacuo at 80 °C for 4 h. Yield: 239 mg (70%). The complex has poor solubility in hydrocarbon and chlorocarbon solvents. IR (mineral oil): 3359, 3260 (m, $\surd_{NH}$). ^{1}H NMR (300 MHz, DMSO-d_6): 7.1−7.8 (40H, PPh), 5.50 (t, J_{H-P} = 24 Hz, 4H, PCH_2P), 1.5 (br s, 4H, NH_2). ^{1}H NMR (250 MHz, CD_3NO_2): 7.2−7.9 (40H, PPh), 4.99 (t, J_{H-P} = 21 Hz, 4H, PCH_2P), 2.1 (br s, 4H, NH_2). ^{31}P{^{1}H} NMR (121 MHz, DMSO): −56.0 (s, J_{P-Pt} = 2588 Hz). ^{31}P{^{1}H} NMR (101 MHz, CD_3NO_2): −54.0 (s, J_{P-Pt} = 2634 Hz).

L_2 = dppe, R = H. A procedure analogous to that given for L_2 = dppm gave the product as a light tan solid. Yield: 85%. Anal. Calcd (found) for $C_{52}H_{52}N_2P_4Pt_2B_2F_8$: C, 44.85 (44.56); H, 3.76 (3.69); N, 2.01 (2.11). IR (mineral oil): 3345, 3253 (m, $\surd_{NH}$). ^{1}H NMR (250 MHz, DMSO-d_6): 7.4−7.8 (40H, PPh), 2.57 (d of m, 8H, PCH_2CH_2P), 1.55 (br s, 4H, NH_2). ^{31}P{^{1}H} NMR (121 MHz, DMSO): 38.2 (s, J_{P-Pt} = 3008 Hz).

L_2 = dppp, R = H. A procedure analogous to that given for L_2 = dppm gave the product as an off-white solid. Yield: 95%. Anal. Calcd (found) for $C_{54}H_{56}N_2P_4Pt_2B_2F_8$: C, 45.65 (45.56); H, 3.97 (4.02); N, 1.97 (1.93). IR (mineral oil): 3342, 3249 (m, $\surd_{NH}$). ^{1}H NMR (300 MHz, DMSO-d_6): 7.3−7.8 (40H, PPh), 2.9 (br, 8H, $PCH_2CH_2CH_2P$), 1.9 (br, 4H, $PCH_2CH_2CH_2P$), 1.4 (br s, 4H, NH_2). ^{31}P{^{1}H} NMR (121 MHz, DMSO): −5.4 (s, J_{P-Pt} = 2860 Hz).

L = PMe_2Ph, R = H. NH_3 gas was bubbled slowly through a stirred suspension of $[(PMe_2Ph)_2Pt(\mu\text{-}OH)]_2(BF_4)_2$ (228 mg, 0.200 mmol) in THF (15 mL). The gas flow was stopped after 10 min, and the mixture was stirred for another 1 h. The reaction mixture was concentrated (3 mL), and hexane was added. The resulting white product was washed with ether and dried at 65 °C in vacuo for 24 h. Yield: 160 mg (70%). IR (mineral oil): 3316, 3111 (m, $\surd_{NH}$). ^{1}H NMR (300 MHz, DMSO-d_6): 7.3−7.9 (20H, PPh), 1.5 (d, J_{P-H} = 10 Hz, 24H, PCH_3), 1.2 (br s, 4H, NH_2). ^{31}P{^{1}H} NMR (121 MHz, DMSO): −14.0 (s, J_{P-Pt} = 2815 Hz).

L_2 = dppm, R = Ph. Aniline (0.093 g, 1.0 mmol) was added to a suspension of $[(dppm)Pt(\mu\text{-}OH)]_2(BF_4)_2$ (684 mg, 0.500 mmol) in THF

(46) Scarcia, V.; Furlani, A.; Longato, B.; Corain, B. *Inorg. Chim. Acta* **1988**, *153*, 67−70.
(47) Siegmann, K.; Pregosin, P. S.; Venanzi, L. M. *Organometallics* **1989**, *8*, 2659.

(40 mL). The reaction mixture was refluxed under nitrogen for 40 min and then cooled to room temperature. The white product was recovered by filtration, washed with THF, and dried at 110 °C in vacuo for 4 h. Yield: 683 mg (90%). Anal. Calcd (found) for $C_{64}H_{56}N_2P_4Pt_2B_2F_8$: C, 49.09 (48.95); H, 3.72 (3.57); N, 1.85 (1.89). IR (mineral oil): 3231 (m, $\surd_{NH}$). ^{1}H NMR (300 MHz, DMSO-d_6): 7.4−7.8 (m, 40H, PPh), 6.2−7.2 (m, 10H, NPh), 4.9 (br m, 4H, PCH_2P), 4.7 (br s, 2H, NH). ^{1}H NMR (250 MHz, CD_2Cl_2): 7.3−7.6 (m, 40H, Ph), 6.14 (m, 10H, NPh), 4.53 (br t, 2H, NH), 4.22 (m, 4H, PCH_2P). ^{1}H NMR (250 MHz, $CDCl_3$): 7.3−7.7 (m, 40H, Ph), 5.9, 5.8 (br m, 10H, NPh), 4.48 (br t, 2H, NH), 4.18 (m, 4H, PCH_2P). ^{31}P{^{1}H} NMR (121 MHz, DMSO): −50.6 (s, J_{P-Pt} = 2813 Hz), ^{31}P{^{1}H} NMR (101 MHz, $CDCl_3$): −47.4 (s, J_{P-Pt} = 2847 Hz).

L_2 = dppe, R = Ph. A procedure analogous to that given for L_2 = dppm gave the product as a light tan solid. Yield: 81%. IR (mineral oil): 3236 (m, $\surd_{NH}$). ^{1}H NMR (300 MHz, DMSO-d_6): 7.2−7.7 (40H, PPh), 6.0−6.5 (m, 10H, NPh), 2.6 (br s, 2H, NH), 2.1, 2.5 (br, 8H, PCH_2CH_2P). ^{31}P{^{1}H} NMR (121 MHz, DMSO): 35.2 (s, J_{P-Pt} = 3130 Hz).

L_2 = dppm, R = *p*-tol. A procedure analogous to that given for L_2 = dppm and R = Ph gave the product as a white solid. Yield: 92%. IR (mineral oil): 3232 (m, $\surd_{NH}$). ^{1}H NMR (300 MHz, DMSO-d_6): 7.3−7.8 (40H, PPh), 5.6−7.1 (m, 8H, NPh), 5.0 (br m, 4H, PCH_2P), 4.9 (br s, 2H, NH), 1.8 (s, 6H, CH_3). ^{1}H NMR (250 MHz, CD_2Cl_2): 7.1−7.7 (m, 40H, Ph), 6.4, 5.8 (br s, 2 × 4H, NC_6H_4Me), 4.57 (br t, 2H, NH), 4.22 (m, 4H, PCH_2P), 1.84 (s, 6H, NC_6H_4*Me*). ^{1}H NMR (250 MHz, $CDCl_3$): 7.3−7.6 (m, 40H, Ph), 6.9, 6.2, 5.9, 5.3 (br s, 4 × 2H, NC_6H_4Me), 4.58 (br t, 2H, NH), 4.22 (t, J = 10 Hz, 4H, PCH_2P), 1.77 (s, 6H, NC_6H_4*Me*). ^{31}P{^{1}H} NMR (101 MHz, DMSO): −49.5 (s, J_{P-Pt} = 2800 Hz). ^{31}P{^{1}H} NMR (101 MHz, CD_2Cl_2): −50 (s, J_{P-Pt} = 2800 Hz). ^{31}P{^{1}H} NMR (101 MHz, $CDCl_3$): −47.5 (s, J_{P-Pt} = 2852 Hz).

L_2 = dppe, R = *p*-tol. A procedure analogous to that given for L_2 = dppm and R = Ph gave the product as an off-white solid. Yield: 75%. Anal. Calcd (found) for $C_{64}H_{60}N_2P_4Pt_2B_2F_8$: C, 49.76 (49.84, 49.77); H, 3.91 (3.95, 3.83); N, 1.81 (1.67, 1.70). IR (mineral oil): 3235 (m, $\surd_{NH}$). ^{1}H NMR (300 MHz, DMSO-d_6): 7.0−7.8 (40H, PPh), 5.8−6.4 (m, 8H, NPh), 3.0 (br s, 2H, NH), 2.1, 2.4 (br, 8H, PCH_2-CH_2P), 2.0 (s, 6H, CH_3). ^{31}P{^{1}H} NMR (121 MHz, DMSO): 35.5 (s, J_{P-Pt} = 3135 Hz).

L_2 = dppm, R = NH_2. A THF (2 mL) solution of NH_2NH_2 (16 mg, 0.50 mmol) was slowly added to a stirred suspension of [(dppm)Pt-(μ-OH)]$_2$(BF_4)$_2$ (378 mg, 0.250 mmol) in THF (10 mL). The reaction mixture was stirred for another 10 min and filtered. All volatiles were removed from the filtrate, and the residue was heated to 100 °C in vacuo for 2 h to remove H_2O. The light yellow product was washed with THF and dried in vacuo. Yield: 331 mg (95%). Anal. Calcd (found) for $C_{50}H_{50}N_4P_4Pt_2B_2F_8$·THF: C, 44.22 (44.53); H, 3.99 (3.99); N, 3.82 (3.71). The presence of THF was confirmed by NMR spectroscopy. IR (mineral oil): 3151, 3231, 3334 (m, $\surd_{NH}$). ^{1}H NMR (300 MHz, DMSO-d_6): 7.2−8.0 (m, 40H, Ph), 5.25 (t, 4H, CH_2), 3.8 (m, 4H, NH_2), 4.0 (m, 2H, NH). ^{31}P{^{1}H} NMR (121 MHz, DMSO): −50.0 ppm (s, J_{P-Pt} = 2660 Hz).

L_2 = dppp, R = NH_2. An procedure analogous to that used for L_2 = dppm gave the product as a light yellow solid. Yield: 70%. IR (mineral oil): 3147, 3248, 3295 (m, $\surd_{NH}$). ^{1}H NMR (300 MHz, DMSO-d_6): 7.1−7.8 (m, 40H, Ph), 2.95 (m, 8H, $PCH_2CH_2CH_2P$), 1.7 (m, 4H, $PCH_2CH_2CH_2P$), 3.3 (m, 4H, NH_2), 1.2 (m, 2H, NH). ^{31}P{^{1}H} NMR (121 MHz, DMSO): −6.3 ppm (s, J_{P-Pt} = 2803 Hz).

L_2 = dppb, R = NH_2. A THF (2 mL) solution of NH_2NH_2 (16 mg, 0.50 mmol) was slowly added to a stirred suspension of [(dppm)Pt-(μ-OH)]$_2$(BF_4)$_2$ (278 mg, 0.250 mmol) in THF (10 mL). The reaction mixture was heated and stirred at 40 °C for 40 min. The mixture was cooled and filtered. All volatiles were removed from the filtrate, and the residue was heated to 70 °C in vacuo for 4 h. The solid product was washed with THF and dried in vacuo. Yield: 208 mg (70%). Anal. Calcd (found) for $C_{56}H_{62}N_4P_4Pt_2B_2F_8$·THF: C, 46.47 (46.58); H, 4.55 (4.72); N, 3.61 (3.34). The presence of THF was confirmed by NMR spectroscopy. IR (mineral oil): 3154, 3253, 3290 (m, $\surd_{NH}$). ^{1}H NMR (250 MHz, DMSO-d_6): 6.8−7.8 (m, 40H, Ph), 2.8, 1.6, 1.4 (m, 16H, $(CH_2)_4$), 2.9 (m, 4H, NH_2), 1.3 (m, 2H, NH). ^{31}P{^{1}H} NMR (101 MHz, DMSO): 7.8 ppm (s, J_{P-Pt} = 2847 Hz).

Amido−Oxo Complexes [(PPh_3)$_4$$Pt_2$($\mu$-O)($\mu$-NHR)]($BF_4$) (3). R = Ph. A solution of $LiNPr^i_2$ (6 mg, 0.056 mmol) in THF (0.5 mL) was added to a white suspension of **1** (L = PPh_3, R = Ph) (96 mg, 0.056 mmol) with stirring. The mixture was stirred at room temperature until a pale-yellow homogeneous solution resulted (ca. 0.5 h). The solution was concentrated to about 1 mL. Ether (2 mL) was added, and the mixture was cooled at −40 °C overnight. The resulting colorless crystals were collected by filtration, washed with ether, and dried in vacuo. Yield: 75 mg (83%). Anal. Calcd (found) for $C_{78}H_{66}BF_4NOP_4Pt_2$: C, 57.33 (56.94); H, 4.07 (3.99); N, 0.86 (0.82). IR (mineral oil): 3294 (m, $\surd_{NH}$). ^{1}H NMR (500 MHz, $CDCl_3$): 2.42 (s, 1H, NH). ^{31}P-{^{1}H} NMR (121 MHz, CH_2Cl_2): 13.33 (d, J_{P-P} = 10 Hz, J_{P-Pt} = 2800 Hz, P trans to O), 10.28 (d, J_{P-Pt} = 3662 Hz, P trans to N).

R = *p*-tol. A procedure analogous to that given for R = Ph gave the product as a white solid. Yield: 81 mg (88%). IR (mineral oil): 3298 (m, $\surd_{NH}$). ^{1}H NMR (500 MHz, $CDCl_3$): 2.40 (s, 1H, NH), 2.38 (s, CH_3). ^{31}P{^{1}H} NMR (121 MHz, CH_2Cl_2): 13.9 (d, J_{P-P} = 10 Hz, J_{P-Pt} = 2840 Hz, P trans to O), 11.0 (d, J_{P-Pt} = 3666 Hz, P trans to N).

R = *p*-Bu^tC_6H_4. A procedure analogous to that given for R = Ph gave the product as a white solid. Yield: 80 mg (88%). Anal. Calcd (found) for $C_{82}H_{74}BF_4NOP_4Pt_2$: C, 58.27 (56.84); H, 4.41 (4.27); N, 0.83 (0.93). IR (mineral oil): 3299 (m, $\surd_{NH}$). ^{1}H NMR (500 MHz, $CDCl_3$): 2.50 (s, 1H, NH), 1.30 (s, Bu^t). ^{31}P{^{1}H} NMR (121 MHz, CH_2Cl_2): 13.9 (d, J_{P-P} = 10 Hz, J_{P-Pt} = 2840 Hz, P trans to O), 11.0 (d, J_{P-Pt} = 3666 Hz, P trans to N).

[(PPh_3)$_4$$Pt_2$($\mu$-O)($\mu$-NHR)](OTf), R = *p*-$NO_2C_6H_4$ (3a). A procedure analogous to that given for **3** (R = Ph) using **1a** gave the product as a pale-orange solid. Yield: 91 mg (90%). Anal. Calcd (found) for $C_{79}H_{65}F_3NO_6P_4Pt_2S$: C, 54.48 (54.17); H, 3.53 (3.53); N, 1.61 (1.91). IR (mineral oil): 3297 (m, $\surd_{NH}$). ^{1}H NMR (500 MHz, $CDCl_3$): 2.80 (s, 1H, NH). ^{31}P{^{1}H} NMR (121 MHz, CH_2Cl_2): 13.2 (d, J_{P-P} = 10 Hz, J_{P-Pt} = 2798 Hz, P trans to O), 10.0 (d, J_{P-Pt} = 3881 Hz, P trans to N).

Deprotonation of Diamido Complexes. [(dppm-H)Pt(μ-NHR)]$_2$ (4). R = H. LiN($SiMe_3$)$_2$ (84 mg, 0.50 mmol) in 2 mL of THF was slowly added to a stirred suspension of [(dppm)Pt(μ-NH_2)]$_2$(BF_4)$_2$ (341 mg, 0.250 mmol) in THF (5 mL). The reaction mixture was stirred for an additional 20 min and filtered. The filtrate was concentrated to 1 mL, and hexane was added. The mixture was stored at −30 °C for 4 h, and the resulting white to pale yellow product was recovered by filtration. Yield: 208 mg (70%). IR (mineral oil): 3359, 3281 (m, $\surd_{NH}$). ^{1}H NMR (250 MHz, CD_2Cl_2): 7.66, 7.35 (m, 40H, Ph), 3.71 (s with satellites, J_{PtH} = 188 Hz, 2H, PCHP), 0.21 (br s, 4H, NH_2). ^{31}P{^{1}H} NMR (121 MHz, THF): −56.4 (s, J_{P-Pt} = 2422 Hz). ^{31}P{^{1}H} NMR (101 MHz, CD_2Cl_2): −57.1 (s, J_{P-Pt} = 2420 Hz).

R = Ph. LiN($SiMe_3$)$_2$ (84 mg, 0.50 mmol) in THF (2 mL) was slowly added to a stirred suspension of [(dppm)Pt(μ-NHPh)]$_2$(BF_4)$_2$ (360 mg, 0.250 mmol) in THF (6 mL). The reaction mixture was stirred for an additional 20 min and then filtered. The filtrate was concentrated to 1 mL and stored at −30 °C for 1 h. The resulting yellow product was recovered by filtration, washed with a small amount of cold THF, and dried in vacuo. Yield: 221 mg, 70% (as a mixture of isomers **A** and **B**). Anal. Calcd (found) for $C_{62}H_{54}N_2P_4Pt_2$: C, 55.52 (55.91); H, 4.06 (4.28); N, 2.09 (1.98). IR (mineral oil): 3283 (m, $\surd_{NH}$). ^{1}H NMR (250 MHz, CD_2Cl_2): 7.5−6.4 (m, Ph), 3.31 (s, 4H, PCHP of **A**), 3.28 (s, PCHP of **B**), 3.09 (br m, NH of **A**), 2.45 (br m, NH of **A**). ^{31}P{^{1}H} NMR (121 MHz, THF): −59.2 (s with satellites, J_{P-Pt} = 2569 Hz, **B**), −59.9 (s with satellites, J_{P-Pt} = 2624 Hz, **A**). ^{31}P{^{1}H} NMR (121 MHz, CD_2Cl_2): −59.4 (s with satellites, J_{P-Pt} = 2540 Hz, **B**), −59.6 (s with satellites, J_{P-Pt} = 2578 Hz, **A**).

R = tol. A procedure analogous to that given for R = Ph gave the product as a yellow solid. Yield: 70% (mixture of isomers **A** and **B**). ^{1}H NMR (250 MHz, CD_2Cl_2): 7.6−6.2 (m, Ph), 3.29 (s, PCHP, **A**), 3.25 (s, PCHP, **B**), 2.98 (br m, NH, **A**), 2.47 (br m, NH, **B**) 2.21 (s, CH_3, **B**) 2.07 (s, CH_3, **A**). ^{31}P{^{1}H} NMR (121 MHz, THF): −58.7 (s with satellites, J_{P-Pt} = 2547 Hz, **B**), −59.4 (s with satellites, J_{P-Pt} = 2584 Hz, **A**). ^{31}P{^{1}H} NMR (121 MHz, CD_2Cl_2): −58.9 (s with satellites, J_{P-Pt} = 2553 Hz, **A**), −59.2 (s with satellites, J_{P-Pt} = 2521 Hz, **B**).

$[(dppm\text{-}H)_2Pt_2(\mu\text{-}NHNH_2)_2Li(THF)_2]BF_4$ (5). $LiN(SiMe_3)_2$ (36 mg, 0.20 mmol) dissolved in 2 mL of THF was added slowly to a stirred suspension of $[(dppm)Pt(\mu\text{-}NHNH_2)]_2(BF_4)_2$ (139 mg, 0.100 mmol) in THF (10 mL) at −30 °C. The reaction mixture was warmed to room temperature, stirred for 10 min, and then filtered. The filtrate was stored at −30 °C for 24 h. The resulting yellow crystals were recovered by filtration. Yield: 109 mg (80%). (Crystals for the X-ray analysis were obtained in this manner.) IR (mineral oil): 3259, 3328 (m, $\sqrt{_{NH}}$). $^{31}P\{^1H\}$ NMR (121 MHz, THF): −56.0 (s, $J_{P-Pt} = 2420$ Hz).

$Li_2[(dppm\text{-}H)Pt(\mu\text{-}NR)]_2$ (6). R = H. LiMe (1.4 M in ether) (0.357 mL, 0.500 mmol) was slowly added with stirring to a suspension of $[(dppm\text{-}H)Pt(\mu\text{-}NHR)]_2$ (297 mg, 0.250 mmol) in THF (10 mL). The resulting homogeneous reaction mixture was stirred for 10 min. All volatiles were removed in vacuo to give the product as a yellow solid. Yield: 208 mg (70%). IR (mineral oil): 3361 (m, $\sqrt{_{NH}}$). $^{31}P\{^1H\}$ NMR (121 MHz, THF): −45.5 (s, $J_{P-Pt} = 2246$ Hz).

R = Ph. LiMe (0.357 mL, 1.4 M in ether, 0.500 mmol) was slowly added with stirring to a suspension of $[(dppm\text{-}H)Pt(\mu\text{-}NHR)]_2$ (316 mg, 0.250 mmol) in THF (10 mL). The yellow homogeneous reaction mixture was stirred for 5 min and was then stored at −30 °C for 24 h. The resulting yellow crystals were collected by filtration. (Crystals for the X-ray and elemental analyses were obtained in this manner.) Yield: 287 mg (90%). Anal. Calcd (found) for $C_{62}H_{52}Li_2N_2P_4Pt_2$: C, 55.04 (55.29); H, 3.87 (3.61); N, 2.07 (2.15). $^{31}P\{^1H\}$ NMR (121 MHz, THF): −48.2 (s, $J_{P-Pt} = 2550$ Hz).

R = tol. A procedure analogous to that given for R = H gave the product as a yellow crystalline solid. Yield: 90%. $^{31}P\{^1H\}$ NMR (121 MHz, THF): −47.5 (s, $J_{P-Pt} = 2503$ Hz).

Crystal Structure Analyses. Crystal data, reflection collection and processing parameters, and solution and refinement data are summarized in abbreviated form in Table 1. A full description is given in the Supporting Information. Crystals were grown as described in the synthesis or Results section above. Crystals of **4** (R = Ph), **5**, and **7** are sensitive to air exposure and were mounted by pipetting crystals and mother liquor into a pool of heavy oil. A suitable crystal was selected and removed from the oil with a glass fiber. With the oil-covered crystal adhering to the end of the glass fiber, the sample was transferred to an N_2 cold stream on the diffractometer and data was collected at the temperatures indicated in Table 1. Crystals of **1** were not air-sensitive (hour time scale) and were mounted on the end of a glass fiber with epoxy and covered with a layer of epoxy.

Acknowledgment. We thank Dr. Paul Raithby for assistance with the structure of **6** and the Department of Chemistry, University of Cambridge, for the use of their library and computer facilities. The Division of Chemical Sciences, Office of Basic Energy Sciences, Office of Energy Research, U.S. Department of Energy (Grant DE-FG02-88ER13880), is gratefully acknowledged for financial support of this work and Johnson Matthey for loans of precious metal salts. Grants from the National Science Foundation provided a portion of the funds for the purchase of the X-ray (NSF-CHE-9011804) and NMR (Grants 8908304 and 9221835) equipment.

Supporting Information Available: An X-ray crystallographic file in CIF format. This material is available free of charge via the Internet at http://pubs.acs.org.

IC981246W